Construction of a femtosecond	mode-locked laser

Contents

1 Introduction	2
1.1 Motivation	2
1.2 Overview	3
2 Principles of Operation	
2.1 Introduction to Lasers	4
2.2 Pulsed Operation	5
2.2.1 Mode-locking	5
2.2.2 Group Velocity Dispersion	11
2.3 Ultrashort pulsed operations. KLM-laser	13
3 Experimental Setup	
3.1 Laser Cavity Design	14
3.2 Materials	15
3.2.1 Active medium and pumping	15
3.2.2 Mirrors	17
3.3 The cavity alignments	18
3.3.1 Prismatic Group Delay Dispersion Compensator	18
3.3.2 Stability zones of the laser	20
3.4 Operating characteristics of the mode-locked laser	22
References	25

The invention of the laser in 1960 stimulated renewed interest in optical physics and gave rise to a number of new research fields. One of them was the field of ultrafast optics, which had the beginning in the mid-1960s with the production of nanosecond (10⁻⁹ s) pulses by the first mode-locked laser. Today, ultrashort pulse generation remains the subject of active research. Rapid progress in this field has led to the creation of practical and useful lasers that can now produce pulses on the femtosecond (10⁻¹⁵ s) time scale. In this work, we make use of these developments to construct a Kerr-lens-mode-locked Ti:sapphire femtosecond laser.

1.1 Motivation

Ultrashort pulse lasers are used in a wide range of areas, both scientific and industrial. The value of ultrashort pulse lasers lies in their time and frequency domain properties. In the time domain, the output consists of high intensity pulses on the femtosecond time scale. In the frequency domain, the pulse train produced by a mode-locked laser consists of a broad spectrum of equidistant modes with a defined phase relationship (Figure 1.1). Ultrashort pulse lasers make it possible to probe nature on the femtosecond time scales, allowing the time-resolved study of a number of ultrafast chemical, biological, and physical processes. For example, such lasers have enabled the triggering and monitoring of ultrafast chemical reactions, the study of relaxation processes and transient phenomena, resolution of molecular dynamics, and the investigation of light-matter interactions [1]. Applications of femtosecond lasers also range from precise materials processing to surgery.

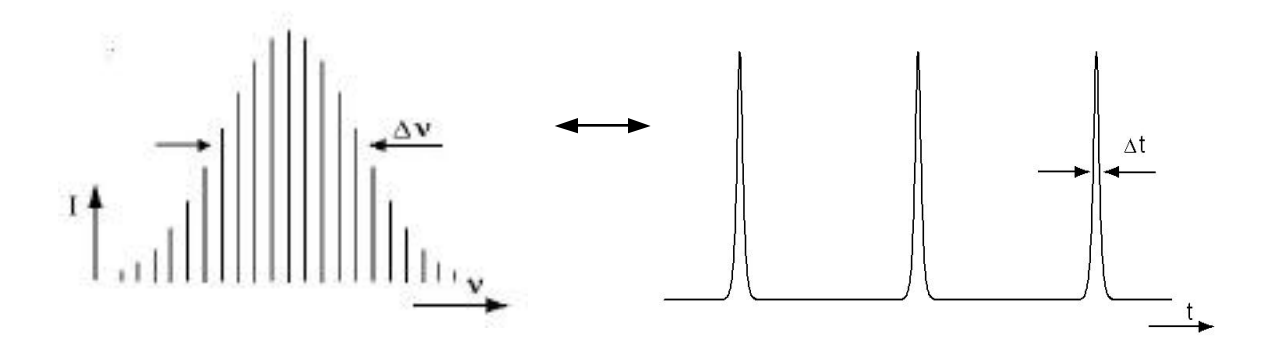


Figure 1.1: An output of a mode-locked laser in frequency and time domains.

Potential applications lie in areas such as communications, high-speed electronics and signal processing [2]. In the frequency domain, the broad spectral comb of equally spaced modes produced by a femtosecond mode-locked laser can be used as a 'ruler' to measure frequency intervals as well as it can be used as a "frequency bridge" to connect distant frequency domains [3,4]. So the ability to generate very short pulses is highly desirable.

The work reported here is a part of the research activities of our group at the University of Pisa. Our group, in collaboration with the frequency standards group of Novosibirsk Institute of Laser Physics (Russia), is currently developing a frequency chain that will be able to coherently link signals of different frequency domains, from optical to radio range. By such chain it will be possible to transfer frequency stability between signals of the different domains. In turn, it will allow us to develop new metrological instruments such as: frequency standards (synthesizers) and frequency counters [5,6]. An optical frequency comb generated by a femtosecond laser is used as a base for development of the frequency chain mentioned above.

1.2 Overview

There are several methods by which pulsed output can be generated, for example Qswitching and mode-locking [7]. By now the most advanced technique for ultarshort pulse generating is Kerr-lens mode- locking in solid-state lasers. This technique can provide sub-10 fs lasing and does not require very complicated design of the laser [8,9]. The essential of this technique consists in the use of Kerr-lens effect in a suitable broadband active medium and support of the intracavity group velocity dispersion compensation [10,11]. So on the way towards construction of a Kerr-lens mode-locked femtosecond laser one has to make a choice of active medium material. That involves finding a laser medium which emits a broad spectrum of radiation covering the desired emission wavelength, and which is also practical to work with. The emission bandwidth of the laser medium is one of the factors determining the duration of the pulses that can be produced by a modelocked laser. It follows from the uncertainty principle: the shorter pulse corresponds to the wider spectra (t 1/). We use the titanium-sapphire crystal that has emission bandwidth covering the range approximately from 650 nm to 1150 nm with the maximum near 800 nm. Ti:sapphire can be easily pumped in blue-green range where some powerful laser sources are available. More over Ti: sapphire has great photo- and thermo-resistance. So it makes Ti: sapphire very attractive for use in mode-locked lasers. Obviously not only active medium provides ability of a laser to generate ultra short pulses. It depends on all intracavity optical elements and on the method used to compensate group velocity dispersion. More particularly these aspects are discussed in the next chapters.

Chapter 2 Principles of Operation

2.1 Introduction to Lasers

First of all let us make very simplified introduction to principles of lasers in order to show the feasibility of mode-locked operating. [7]

The mechanism of laser action relies on stimulated emission. This is a process whereby the interaction of a photon with an atom in an excited state results in the de-excitation of the atom, and the emission of a second photon that is coherent with the first one (Figure 2.1). The energies of the involved photons are equal to the energy difference between the two states involved in the lasing transition. Three essential elements are required in the construction of a laser. These are: an active medium in which stimulated emission takes place, a pumping process to create a population inversion, and optical feedback elements (mirrors (Figure 2.2)). So the radiation undergoes many trips through the active medium and is amplified on each pass. The lasing is possible when the round-trip gain of the active medium exceeds the round-trip losses of the cavity.

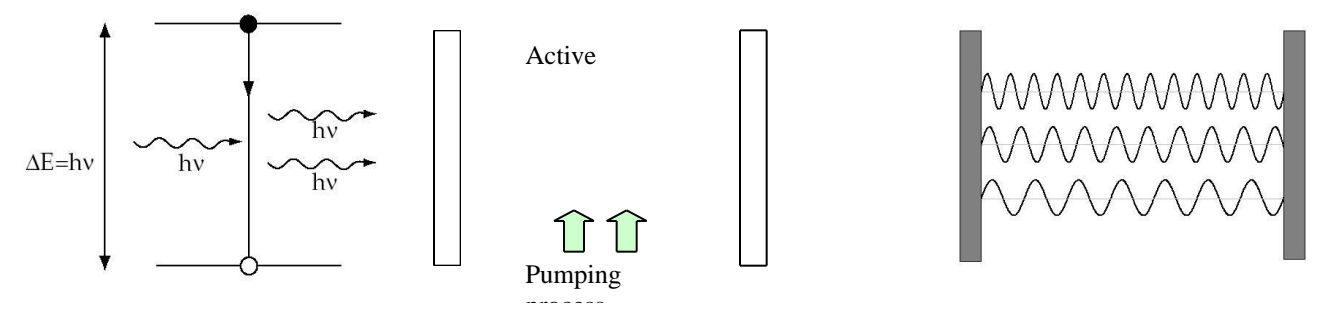


Fig 2.1: Stimulated emission

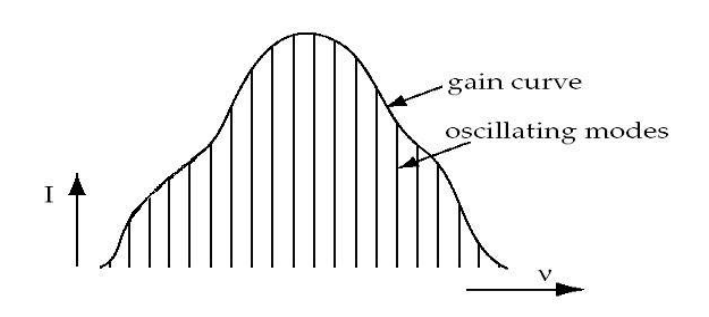
Fig 2.2: Typical laser elements

Fig 2.3: Longitudinal modes

A laser may oscillate in more than one mode simultaneously, that is, its output may consist of light of a number of frequencies (Figure 2.3). The axial (longitudinal) modes supported by the laser cavity are those that satisfy the boundary condition, that is, allowed modes are those for which the cavity length is an integer number of half wavelengths. This requires that,

$$i_q = q \frac{c}{2L}$$
 or $\frac{\ddot{e}}{2} = \frac{L}{q}$ (2.1)

where q is an integer, c is the speed of light, and L is the length of the cavity. From this, it can be seen that the spacing between axial cavity modes is equal to $\frac{c}{2L}$, the reciprocal of the cavity round-trip time. It is important to note that although all modes that satisfy this condition are supported by the cavity and can oscillate, output will only be seen in those modes for which the gain of the cavity exceeds the losses (Figure 2.4).



I(t)

Figure 2.4: Oscillating modes

Figure 2.5: Fluctuating output of a multi-mode laser.

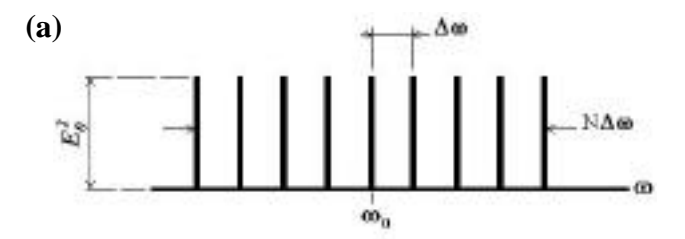
In a general continuous wave multi-mode laser, the modes will oscillate independently of each other and will have random phases relative to one another. Since the total electromagnetic field at any point inside the cavity is given by the sum of the fields of the oscillating modes, the output of such a laser will be noise-like, fluctuating in intensity due to interference between the modes (Figure 2.5). However it is possible to manipulate the phases of the modes to obtain a more useful output, with a technique known as mode-locking.

2.2 Pulsed Operation

2.2.1 Mode-locking

A multi-mode laser is said mode-locked if its modes have a well-defined and fixed phase relationship. If the phases are locked in such way that there is a constructive interference between the modes at an instant and a destructive interference at other times, the output will appear as a pulse. It is instructive to consider a simple example of mode-locking in which all oscillating modes have equal amplitude (Figure 2.6,a). The electromagnetic field due to 2n+1 equally spaced modes is given by:

$$E(t) = \sum_{q=-n}^{n} E_q e^{i\left[(\omega_0 + q \cdot \omega)t + \varphi_q\right]}$$
(2.2)



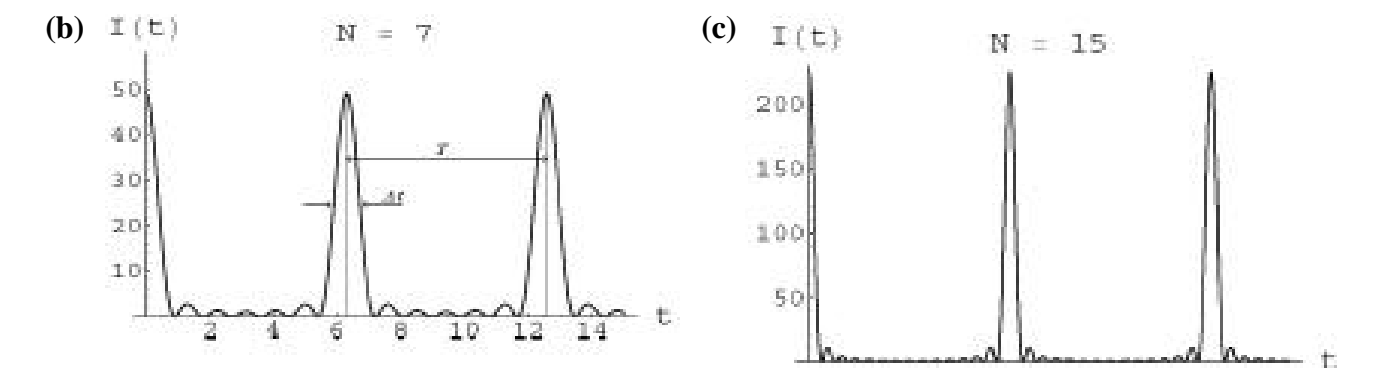


Figure 2.6: Mode-locked output for the equal-amplitude approach: (a) spectrum; (b, c) the output in time domain (variation of intensity with time) for different numbers (N) of involved modes.

Where we have summed over all possible modes. E_q is the amplitude of the qth mode, ω_0 is the frequency of a central mode, $\Delta\omega$ is the (angular) frequency spacing between modes, and φ_q is the phase of the qth mode. In the case of equal amplitudes (E_θ) and locked phases (φ_q - φ_{q-1} =const), considered here, this sum becomes:

$$E(t) = E_o e^{i\omega_0 t} \int_{q=-n}^{n} e^{iq \cdot \omega t}$$
(2.3)

Then, it can be written as $E(t) = A(t)e^{i\omega_0 t}$, where: $A(t) = E_0 \int_{q=-n}^{n} e^{iq + \omega t}$. (2.4)

So we have got an amplitude-modulated wave oscillating at the central mode frequency (ω_0). In fact the expression for A(t) contains a geometrical progression. From this we can convert it to another form and write down the intensity as a function of time in the following way:

$$I(t) \quad [A(t)]^{2} = \frac{\sin^{2}[(2n+1) \omega t/2]}{\sin^{2}(\omega t/2)}$$
 (2.5)

This function is a periodic one, with strong peaks (pulses) equally spaced by very weak subsidiary peaks (Figure 2.6, b, c). From the analysis, one can show several other important properties of this function. The pulse duration decreases, and its amplitude increases, as the number of modes increases; the period of this function (time spacing between pulses) is $T = 2\pi/\omega$; The pulse duration Δt can be approximately given as $t = 2\pi/(2n+1) = 1/\nu$, where is a full width of the generation band. From this simple example, it becomes clear that mode-locking results in a periodic intensity pulse, in contrast to the noisy, fluctuating output of the non-mode-locked case.

Let us now consider a continuum of oscillating modes with non-equal amplitude distribution. This is a valid approximation for real ultrashort pulse lasers, where there is very large number of closely spaced oscillating modes and their amplitude distribution usually has a gaussian-like profile (Figure 2.7, a).

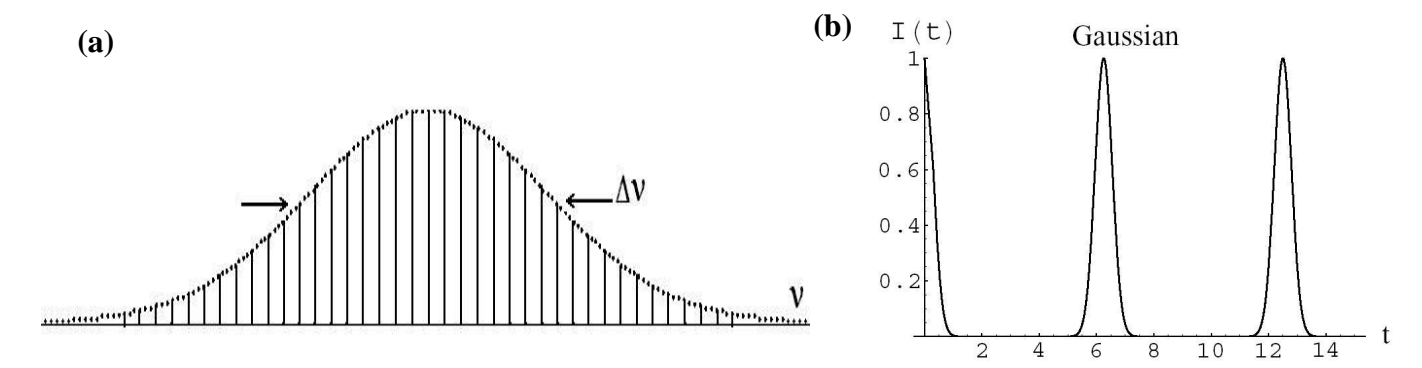


Figure 2.7: Mode-locked output for the gauss-approximation of the amplitude distribution: (a) spectrum, (b) the output in time domain (variation of intensity with time).

In this case the expression for A(t) (see the equation 2.4) must be written as $A(t) = \int_{q=-n}^{n} E_q e^{iq} \, \omega t$. Then it can be treated as an integral, and the limits may be taken to be infinity; provided that the amplitude E_n is appropriately zero in the limits:

$$A(t) = E_q e^{iq \cdot \omega t} dq (2.6)$$

This integral is a Fourier transform. So, in the time domain the amplitude of a multi-mode output is given by the transform of the amplitude distribution of modes in the frequency domain. For instance, the mode-locking of a continuum of oscillating modes with a gaussian distribution of amplitude will result in gaussian pulses (Figure 2.7,b):

Figure 2.7,6):
$$[A(t)]^{2} \sim \exp -\ln 2 \frac{2t}{t_{0.5}}$$
 (2.7)

The duration of the half-height of such pulses is given by:

$$t_{0.5} = \frac{2\ln 2}{\pi \, \text{ y}} = \frac{0.441}{\text{y}} \tag{2.8}$$

In principle, the relation between the pulse duration and the width of oscillating spectra is

$$t = \frac{\kappa}{\nu},\tag{2.9}$$

where k is a factor of the spectrum shape. However this is valid provided that the mode-locking is considered for the simple phase relationship noted above ($\varphi_{\mathbf{q}}$ - $\varphi_{\mathbf{q}-\mathbf{1}}$ =**const**). In this case generated pulses are called "transform limited pulses". The duration of such pulses is minimal and is defined

by the width of oscillating spectra.

There are several techniques by which mode-locking can be achieved. In general, these techniques rely on some forms of periodic amplitude modulation of the multi-mode laser radiation. If the modulation period corresponds to the round-trip time around the cavity $T = \frac{2L}{c}$ or, by other words, the modulation frequency corresponds to the allowed frequency spacing between axial cavity modes, mode-locking can occur. The process leading to mode-locking can be explained in either the time domain or the frequency domain. In the frequency domain, we can consider that all the involved modes under modulation develop individual sidebands. The sidebands of any mode lie close to its neighboring modes, provided that the frequency of modulation is close to the frequency spacing of oscillating laser modes. In turn the sidebands can couple to the neighboring modes near which they fall, leading to the phase-locking of an axial mode to its neighbors.

Practically, the methods of achieving mode locking can be split into three main techniques: active mode-locking, passive mode-locking, and self-mode-locking:

Active Mode-Locking

This principle essentially involves placing a very fast shutter in the laser cavity. Mode locking takes place if the shutter opens only for a very short period of time, every time the light pulse makes a complete roundtrip in the cavity. It is, however, not necessary to fully close the shutter. A sinusoidal-modulated transmission of the shutter, provided that the modulation frequency is equal to the intermode frequency separation $\Delta\omega = \mathbf{c}/2\mathbf{L}$, also causes the attenuation of any radiation not arriving at the time of peak transmission. This active Q-modulation can be achieved with different kinds of electro-optical or acousto-optical modulators placed inside the laser cavity.

Passive Mode-Locking

Passive mode locking is obtained by inserting a saturable absorber into the laser cavity, preferably close to one of the mirrors. A saturable absorber is a medium whose absorption coefficient decreases as the intensity of light passing through it increases; thus it transmits intense pulses with relatively little absorption and absorbs weak ones. When a saturable absorber is used to mode lock a laser, the laser is simultaneously Q-switched. For example, a saturable dye can mimic

the fast shutters used for active mode locking, provided that the pulse has a sufficiently large irradiance to allow it to saturate the absorber each time it passes through. The recovery time must be shorter than the roundtrip time; otherwise multiple pulses could form. Initially, the laser medium emits spontaneous radiation, which gives rise to random temporal fluctuations of the energy density. Some of these fluctuations may be amplified by the laser medium and grow in irradiance to such an extent that the peak part of the fluctuation is transmitted by the saturable absorber with little attenuation. The low power parts of the fluctuation are more strongly attenuated and thus a high-power pulse can grow within the cavity. Adjusting the concentration of the dye within the cavity may cause an initial fluctuation to grow into a narrow pulse traveling within the cavity, producing a periodic train of mode-locked pulses.

Self-Mode-Locking (Kerr-lens-mode-locking)

In this project we make use of a self-mode-locking mechanism that relies on the optical Kerr effect inside of the active medium. The optical Kerr effect is a third-order, non-linear effect which results in a change induced in the refractive index of a material by applied high-intensity electric fields [12]. The behavior of the refractive index under the Kerr effect is intensity dependent and can be described by:

(2.10)

$$n(I)=n_0+n_2I$$
,

where n_o is the linear refractive index, n_2 is the nonlinear refractive index coefficient, and I is the instantaneous beam intensity. For typical solid-state materials, the nonlinear index n_2 is on the order of several 10^{-16} cm²/W. So it becomes considerable only for the high-intensity light pulses.

In a pulsed laser the refractive index n of active medium is proportional to the time- and space-dependent intensity $I(t, \vec{x})$ of the pulsed radiation. Therefore, the expression 2.10 can be written as:

$$n(t, \vec{x}) = n_0 + n_2 I(t, \vec{x})$$
 (2.11)

The radiation pulse, propagating through such medium, experiences a greater refractive index for the central part, which is the most intense. So the first conclusion one may do is that the central part of the beam travels at a lower velocity than the peripheral part. The index change causes a temporal delay or phase shift for the most intense parts of a beam. Assuming Gaussian spatial and temporal profiles of pulses, the effects caused by the longitudinal and transverse index change are shown on

the Fig.2.8. Retardation of the most intense part of a plane wave front transversely acts like a focusing lens, whereas along the axis of propagation, the Kerr effect retards the center of an optical pulse. The longitudinal effect produces a red shift of the leading part of the pulse, and a blue shift in the trailing part and has also been named self-phase modulation (SPM). It is important to note that SPM generates extra bandwidth, that is, it spectrally broadens the pulse [10,11].

The formation of the Kerr-lens causes the beam to undergo "self-focusing" when it passes through the medium. Since the degree of self-focusing is intensity dependent, there exists the possibility of introducing an intensity dependent loss mechanism in the cavity. Mode-locking can then occur.

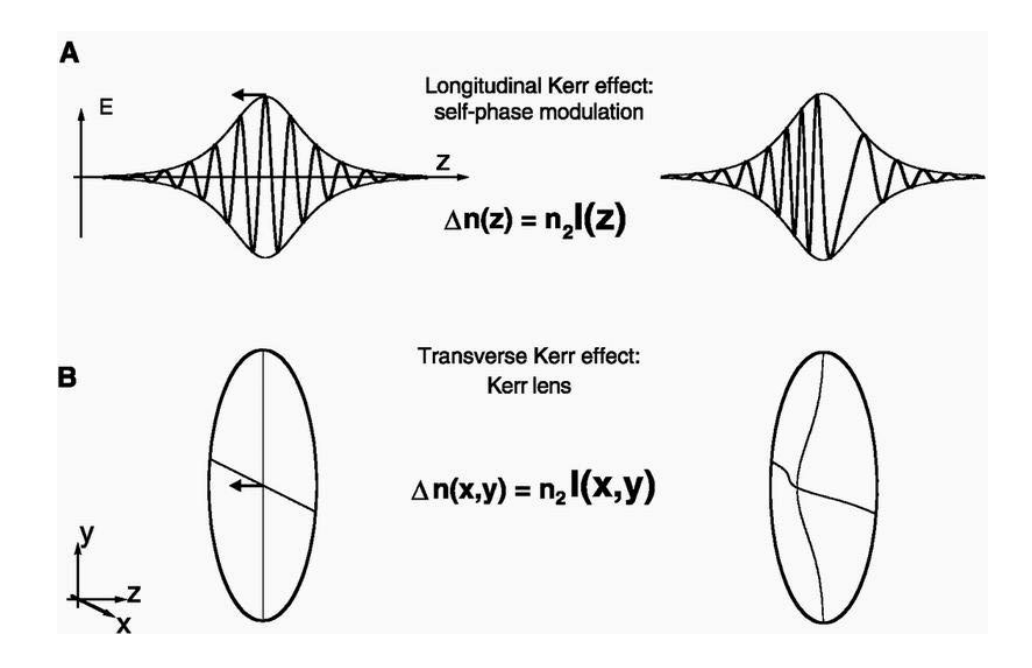


Fig.2.8. The Kerr effect gives rise to an increase of the refractive index with intensity, causing a retardation of the most intense parts of a pulse. In its longitudinal form (**A**), the Kerr effect causes self-phase modulation; in its transverse form (**B**), a nonlinear lens is formed in the central part of the beam profile.

To obtain these two methods can be used. Since "self-focusing" results in a spatial change of the beam, one method is to introduce an aperture or slit into the cavity. The size of the aperture is

chosen so that a sufficiently self-focused beam can pass the aperture without attenuation, due to the smaller beam size, whilst a less focused beam will undergo attenuation due to diffraction losses. Use of a physical aperture, called a 'hard' aperture, can thus create an intensity-dependent loss mechanism that favors higher intensity beams. This mechanism acts like a fast saturable absorber. A second method is to use 'gain-guiding'. No additional intracavity elements are needed for this. Appearance of a Kerr-lens inside the active medium results in a local reshaping of the laser modes. Firstly, under certain conditions, it can improve overlapping of the generated radiation with the pump beam, and thus can result in an increase in gain ('soft' aperture mechanism). Secondly, appearance of a Kerr-lens can be used to eliminate artificially induced cavity misalignments. So, by these mechanisms a greater Q-factor is provided for the more intense pulse by the intensity-dependent gain or intensity-dependent losses, respectively. [13,14]

2.2.2 Group Velocity Dispersion Compensation

In the previous section it was shown that output of a multi-mode laser can result in regular pulse train; provided that a mechanism of mode-locking is involved in the construction of the laser. However, in order to successfully generate ultrashort pulses, the modes must retain their phase relationship over all the time so that the mode-locking is stable. This requires that all modes experience the same round-trip cavity time, or, equivalently, that the optical length of the cavity is independent of frequency (as it was considered in the equation 2.1). In general this will not be the case, due to the presence of frequency dependent dispersion in the cavity materials, that is, n= $function(\omega)$. This results in different propagation speeds for the different frequency components of the pulse. That is, the pulse will experience group velocity dispersion (GVD) or, by other terms, group delay dispersion (GDD), as it travels through the cavity. This will typically lead to temporal broadening of the pulse, limiting the generation of ultrashort pulses, or even, will disable the mode-locking [10,11]. Indeed, in the time domain the complex electric field of light pulse can be completely characterized by Fourier transform of its frequency domain representation:

$$\boldsymbol{E}(t) = \int_{-\infty}^{\infty} \widetilde{\boldsymbol{E}}(\omega) \exp\left[-i\omega t\right] d\omega \tag{2.12}$$

where _(t) and _(_) are terms of the complex electric field in time and frequency domain, respectively. The frequency domain description consist of spectral amplitude and phase distributions:

$$\widetilde{E}(\omega) = \left| \widetilde{E}(\omega) \right| \exp\left[-i\phi(\omega) \right]$$
 (2.13)

The continuous phase distributions $(_)$ can be developed as a power series around the central frequency $__0$, assuming the phase varies slowly with frequency:

$$\phi(\omega) = \phi(\omega_0) + \phi'(\omega_0)(\omega - \omega_0) + \frac{\phi''(\omega_0)}{2}(\omega - \omega_0)^2 + \frac{\phi'''(\omega_0)}{6}(\omega - \omega_0)^3 + \dots$$
(2.14)

This expansion is motivated by an intuitive interpretation of the derivatives of the phase in terms of time domain quantities. Assuming some phase profile imparted by a dispersive optical element, the first term in the series is the relative phase at the frequency _0 (phase at origin), the first derivative is the group delay (GD) and the second derivative gives group delay dispersion (GDD). As the higher order derivatives usually give very small contribution, the third- and fourth-order dispersion (TOD and FOD) usually are neglected. Figure 2.9 shows the effect of dispersion on a Gaussian pulse traveling through a piece of glass. There are two points to notice. Firstly, the center of the pulse is delayed with respect to a pulse traveling in a non-dispersive medium. This is due to the group delay, which is not a broadening effect. Secondly, normally-dispersive medium, like glass, impose a positive frequency sweep or "chirp" on the pulse meaning that the blue components are delayed with respect to the red and the pulse becomes broadened one. This is due to presence of the positive GDD. It is possible to show that the output pulse is broadened with respect to the input Gaussian pulse by a factor [15]:

$$\frac{\tau_{out}}{\tau_{in}} = \sqrt{1 + \frac{\text{GDD}^2}{\tau_{in}^4} 16(\ln 2)^2},$$
(2.15)

Undesirable group velocity dispersion can be compensated in a number of ways, by installing additional intracavity elements, which give a GVD of opposite sign. In a standard four-mirror cavity for Kerr-lens mode-locked lasers, group velocity dispersion compensation is generally achieved by introducing a prism pair into the cavity. The first prism acts to angularly disperse the incident beam, whilst the second recollimates the spectral components (Figure 2.10). The angular dispersion results in negative GVD that is proportional to the prism separation distance. This

counteracts the positive GVD accumulated by the beam in the traveling through the other cavity materials. There is also a positive GVD component, arising from the path through the prism material. The total GVD of the prism sequence can be manipulated by adjusting the prisms spacing and intraprism path length [15].

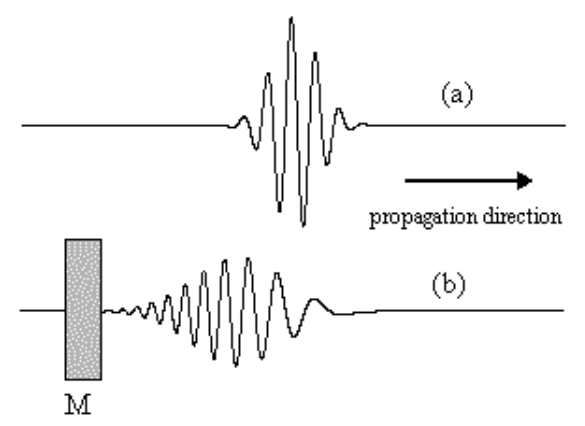


Figure 2.9. Schematic diagram of the electric field of (a) a Gaussian pulse propagating in a non-dispersive medium and (b) the same pulse after traveling through a positively-dispersive medium.

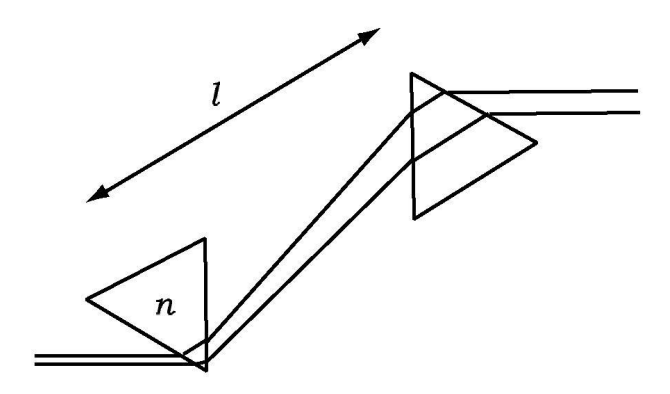


Figure 2.10: A prism pair for group velocity dispersion compensation.

2.3 Ultrashort Pulsed Operation. KLM-laser.

Since we can provide our construction of a laser with all elements, described above, such as: a broadband active medium, a suitable mechanism of mode-locking, GVD-compensation, we can already expect for an output consisting of ultrashort pulses. However, to get minimum pulse duration we must also involve self-phase modulation (SPM) mechanism, mentioned in the previous chapter. It is important to note that SPM, induced by Kerr-nonlinearity in active medium, generates extra bandwidth that spectrally broadens the pulse. SPM alone does not modify the pulse envelope, but a much shorter pulse can be created with the extra bandwidth generated, as it follows from the Fourier transform of the wider spectrum. In the time domain SPM gives a red shift of the leading part of the pulse, and a blue shift in the trailing part (Fig.2.8, a). To exploit the broadened bandwidth for the generation of a shorter pulse, the red and blue components in the temporal wings of the pulse have to be temporarily delayed and advanced, respectively. A careful balance between frequency dependence given by dispersion and time dependence given by Kerr-nonlinearity of the refractive index n is needed for high-efficient compression of a pulse [10]. Since it is provided, laser acting with use of SPM-mechanism can result in extremely short (few-cycles) pulses [9]. The bloc-diagram, including all mechanisms of such Kerr-lens mode-locked (KLM) laser is shown on the Fig.2.11.

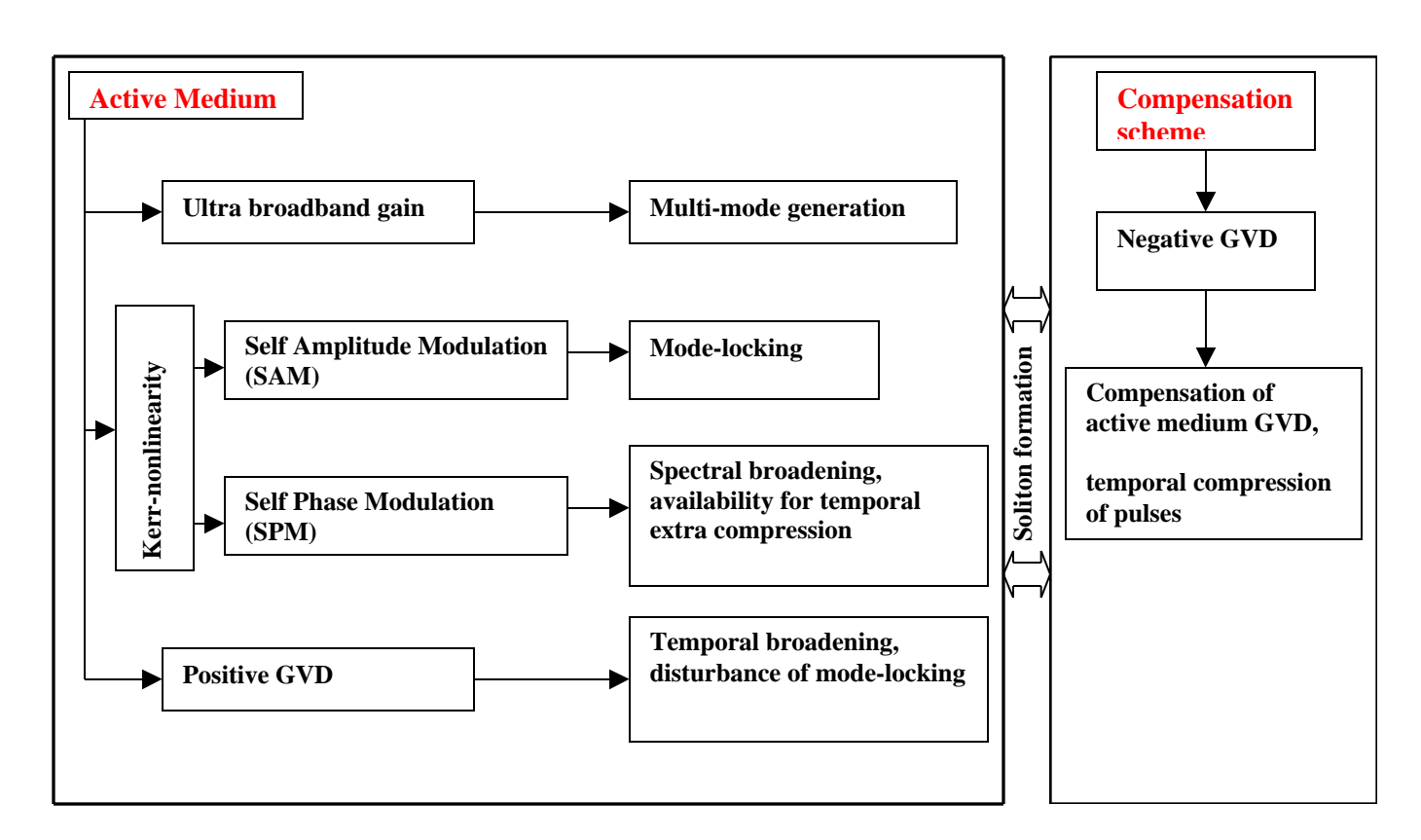


Fig.2.11. Block diagram of a femtosecond KLM lasers.

3.1 Laser Cavity Design

The laser cavity design is based on a standard four-mirror Z-folded resonator for a solid-state Kerr-lens mode-locked laser [8]. Such a cavity consists of a Brewster-cut active medium, folding spherical mirrors, and two arms bounded by plane mirrors (Figure 3.1). One of the arms contains a prism pair for group velocity dispersion compensation. One of the plane mirrors acts as an output coupler

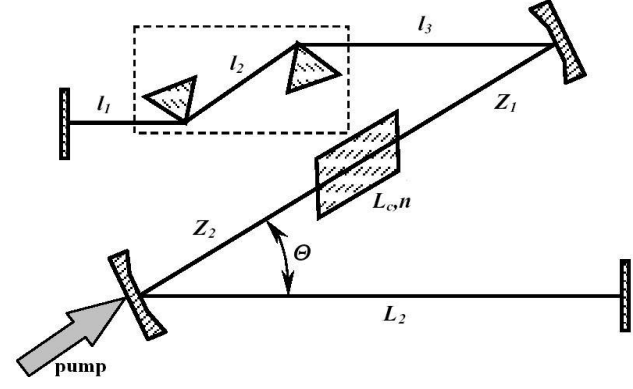


Figure 3.1. Schematic diagram of a standard four-mirror Z-folded resonator.

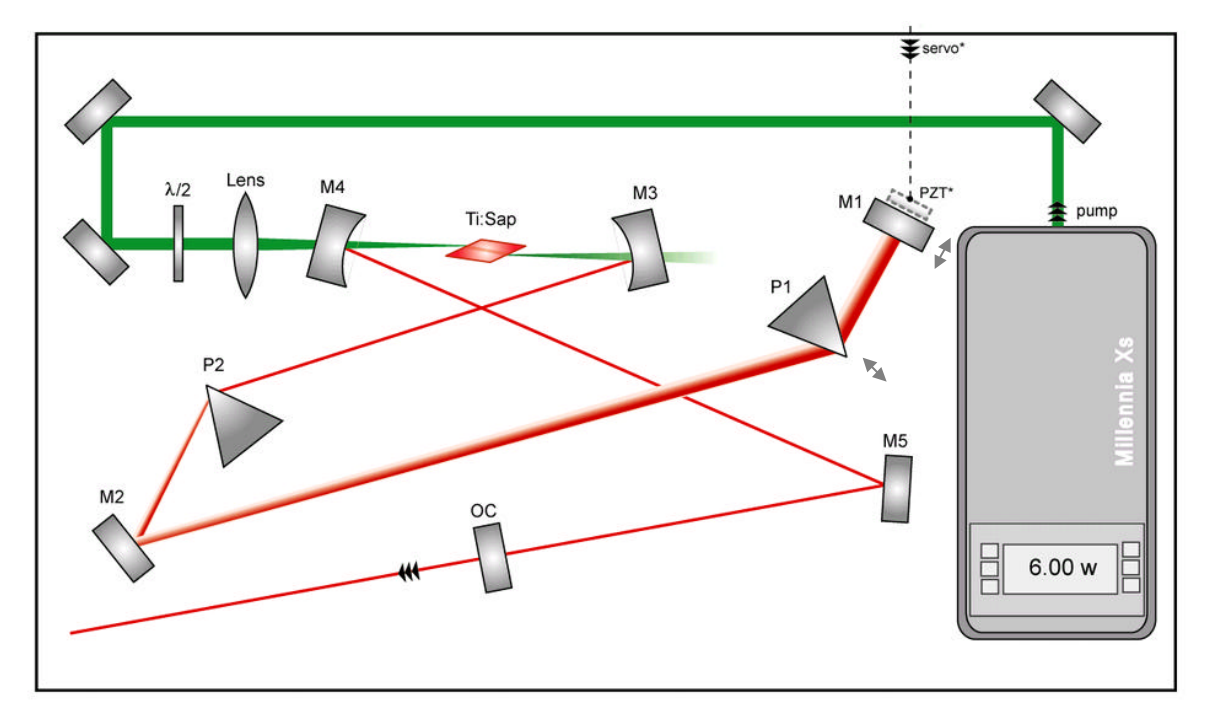


Figure 3.2. Schematic diagram of the laser:

Ti:Sap, Titanium-Sapphire crystal; **M3**, **M4**, HR concave mirrors; **M1**, **M2**, **M5**, HR plane mirrors; **P1**, **P2**, fused silica prisms; **OC**, output coupler; **PZT**, piezotranslator (*option);

In our construction of the cavity we also had to employ two additional folding plane mirrors in order to avoid excessive dimensions of the laser (Figure 3.2). Although, in fact, the cavity now consists of six mirrors, it can be considered as a four-mirror resonator, described above.

3.2 Materials

3.2.1 Active medium and pumping

The active medium used in the laser is a Titanium-ion doped sapphire crystal (Ti^{3+} : Al_2O_3). This is a vibronic laser medium, as there is strong coupling between the vibrational energy levels and the electronic energy levels of the Ti^{3+} active ions (Figure 3.3). The vibronic nature of Ti^{3+} : Al_2O_3 leads to broad absorption and emission spectra (Figure 3.4). [7]

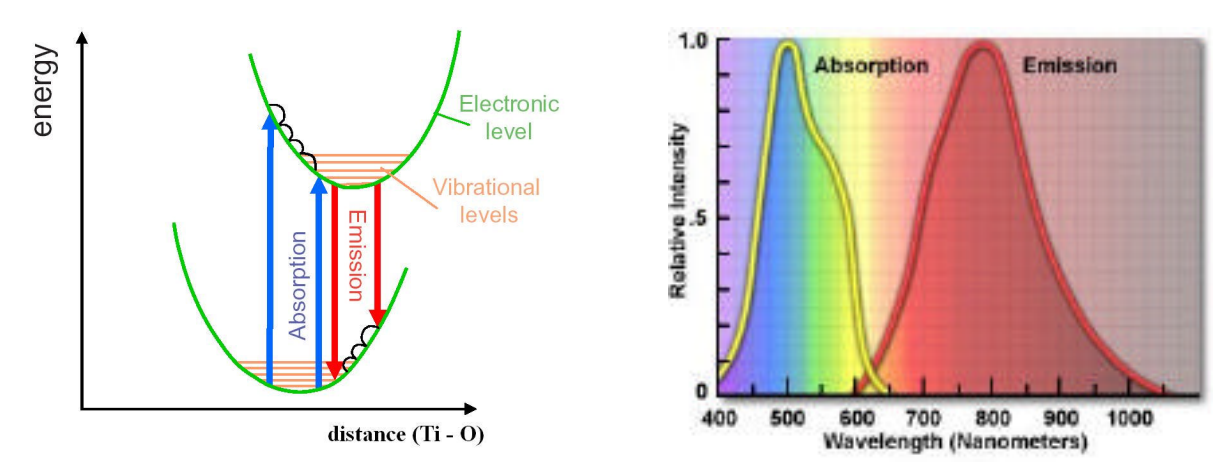


Figure 3.3: The energy levels diagram for Ti:sapphire

Figure 3.4: Ti:sapphire absorption-emission spectra

The crystal has a hexagonal structure with Aluminum in the center and Oxygen atoms in the vertices; after doping, some Al^{3+} ions are replaced by Ti^{3+} ions. Crystalline field perturbs the electronic energy level of Titanium ion (Figure 3.5). Ti:sapphire is a four level laser medium; at room temperature only the lowest vibrational level (T_2 , T_2) is populated since the energy spacing between excited levels is larger than KT. After exciting the transition to the electronic states (T_2 , T_2) the electrons relax quickly to the level (T_2 , T_2) and then to the lower levels (T_2 , T_2); the cycle is then closed by the fast transition to the fundamental level; all these transitions follow the Franck - Condon principle [7]. Laser action happens during the transition from (T_2 , T_2) to (T_2 , T_2). The lifetime of upper laser level is about 3.2 T_2 s. The most important laser properties of the used

Ti:sapphire crystal are presented in the table 1. It must be stressed that the equilibrium distances of the system Ti-O in the fundamental level are very different with respect to the distances in the excited level. This causes a big separation between emission and absorption bands and their large width. The absorption band centered at 490 nm makes it suitable for variety of laser pump sources - argon ion, frequency doubled Nd:YAG and YLF, copper vapor lasers. We use a frequency-doubled diode-pumped Nd:YVO₄ laser, (Spectra-Physics Millennia Xs). This laser can provide high power (up to 10 W) of high stable pumping radiation at wavelength of 532 nm in TEM₀₀ spatial mode.

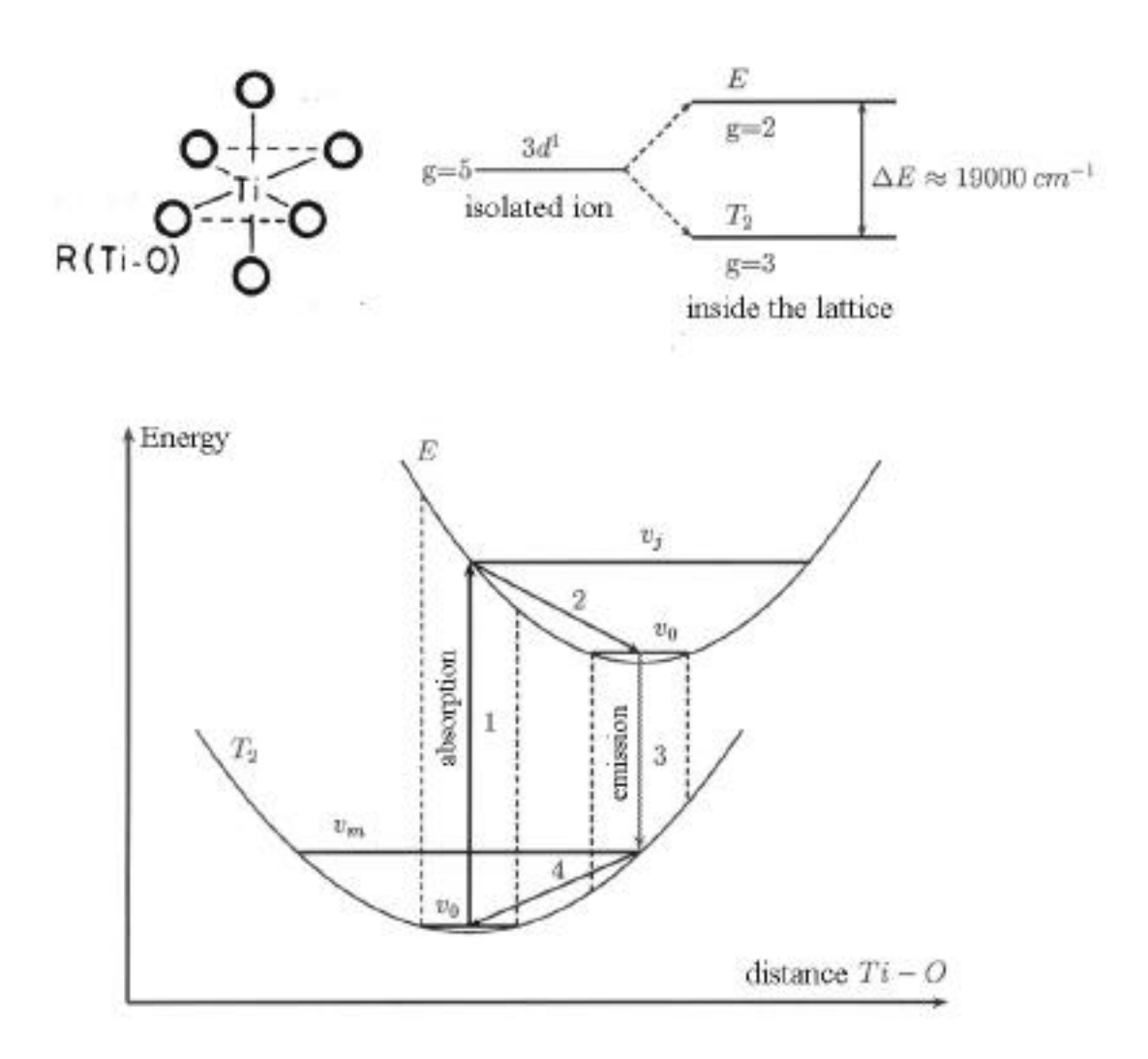


Figure 3.5: The diagrams showing the feasibility of laser use of Ti^{3+} : Al_2O_3 crystal: (a) Titanium ion hosted by the lattice; (b) states of 3d-electron of Ti^{3+} ion; (c) energy levels and transitions involved in the lasing.

Table 1: Active medium physical and laser properties:

Chemical formula	Ti ³⁺ : Al ₂ O ₃
Crystal structure	Hexagonal
Lattice constants	a = 4.748, c = 12.957
Laser action	4-Level Vibronic
Fluorescence lifetime	3.2 _sec (T = 300 K)
Tuning range	660-1050 nm
Absorbtion range	400-600 nm
Emission peak	795 nm
Absorption peak	488 nm
Refractive index	1.76 @ 800 nm

Laser rod specification:

Orientation	Optical axis C normal to rod axis
Size	5 mm long
End configurations	Brewster/Brewster ends
Ti ₂ O ₃ concentration	0.15 wt %
Absorption (_ @ 532 nm)	2.5 cm ⁻¹

Given the low absorption cross-section and (compared to dye laser materials) a relative low gain cross-section, a long gain medium is required to ensure efficient pumping and overall gain. As a result of this length, the crystal must be pumped collinearly to obtain the best overlap between pump and resonator mode. An anti-reflection coated lens is used for focusing the pump beam in the Ti:sapphire crystal. The polarization of the pump beam is rotated by the phase plate _/2. The polarization of the laser mode is parallel to the optical table and governed by the lossless propagation through the Brewster surfaces of the crystal and the prisms. Moreover, the Ti:sapphire rod may act as a birefringent filter in the cavity and thus works as a mode selector. Only the modes that have the correct polarization orientation will propagate without any losses. Setting of the c-axis of the sapphire crystal parallel to the polarization direction of the circulation radiation, results in the lossless propagation over the whole accessible gain bandwidth (fig.3.6). Therefore careful alignment of the crystal axis is crucial to sustain the broadband mode-locked operation of the laser.

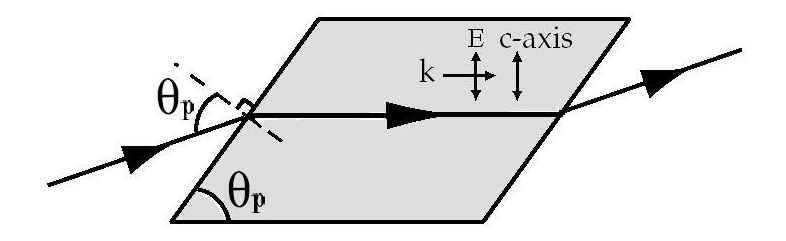


Figure 3.6: Geometry of the Brewster-cut crystal with $\mathbf{E} \parallel \mathbf{c}$.

To avoid the accumulation of heat in the Ti:sapphire crystal, the supporting mount is cooled by running tap water. Under normal operation conditions, the temperature of the crystal is slightly higher than room temperature, which furthermore prevents the accumulation of condensation on the crystal.

3.2.2 Mirrors

In the laser construction we make use of dielectric ultrabroad-band mirrors. The high reflectivity band of the mirrors spans the range from, approximately, 830 nm up to 980 nm. Nevertheless, laser generation appears on the short-wave side of the span as it is closer to the wavelength of Ti:sapphire emission peak. Obviously, all loss-minimizing Brewster angles of optical elements are also performed at that wavelength. The concave mirrors have a radius of curvature of 100 mm. These mirrors are transparent for the pumping radiation. Moreover, the rear side of the mirror M4 (see figure 3.2) has an anti-reflection coating for the pump wavelength of 532 nm. For the output couplers, different values for the transmission coefficient can be used, ranging from T=1% up to T=20%. In the presented design, we make use of T=4% and, alternatively, T=10% output couplers.

3.3 The cavity alignments

3.3.1 Prismatic Group Delay Dispersion Compensator

The negative group delay dispersion (GDD) element, necessary to sustain the pulse generation is formed by a double-pass prism arrangement. The Brewster angle fused silica prisms are aligned for minimum deviation. The choice of fused silica is based on the fact that the prism pair can compensate the positive GDD of a 5 mm long Ti:sapphire crystal with a reasonable prism separation distance. Furthermore, in comparison with other types of glasses, fused silica exhibits a low amount of third-order dispersion.

Indeed, with the geometry shown on the Figure 3.7 for two prisms, and taking $n_0 = (dn/d_{-})_{0}$ and $n_0 = (d^2n/d_{-})_{0}$, where n is the refractive index of the prisms and n_0 is the pulse central wavelength, we can obtain GDD by [15]:

$$\varphi_p = \frac{2\lambda_0^3}{\pi c^2} - Ln_0^2 + e \frac{n_0 n_0}{1 + n_0^2} + n_0^2 1 - \frac{1}{n_0^2 (1 + n_0^2)}$$
(3.1)

Here c is the light velocity in the vacuum, L the distance BC between the prisms, and e the quantity defined in Fig.3.7 by e=AB+CD. As a comparison, we recall the expression of the dispersion introduced by a length l of a transparent medium [15]:

$$\varphi_m = \frac{\lambda_0^3}{2\pi c^2} n_0 l \tag{3.2}$$

Looking at these different expressions of ____, one can see that if usual materials (including Ti:sapphire) present a positive dispersion (as n_0 _>0) it can be compensated by prisms with a sufficient spacing between them (_p_<0 if L is large enough).

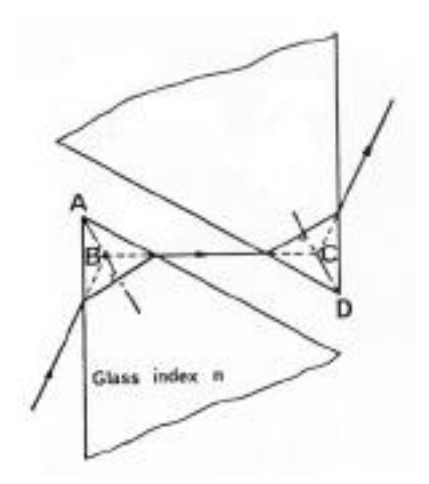


Figure 3.7: Geometrical construction to obtain the optical path for two prisms. Note that L=BC and e=AB+CD.

To perform the calculations of GDD, we treated the expressions 3.1 and 3.2 with the Sellmeir equation for refractive index. We have computed that a prism separation of 62 cm is needed. The result curves of dispersion are shown in the figure 3.8.

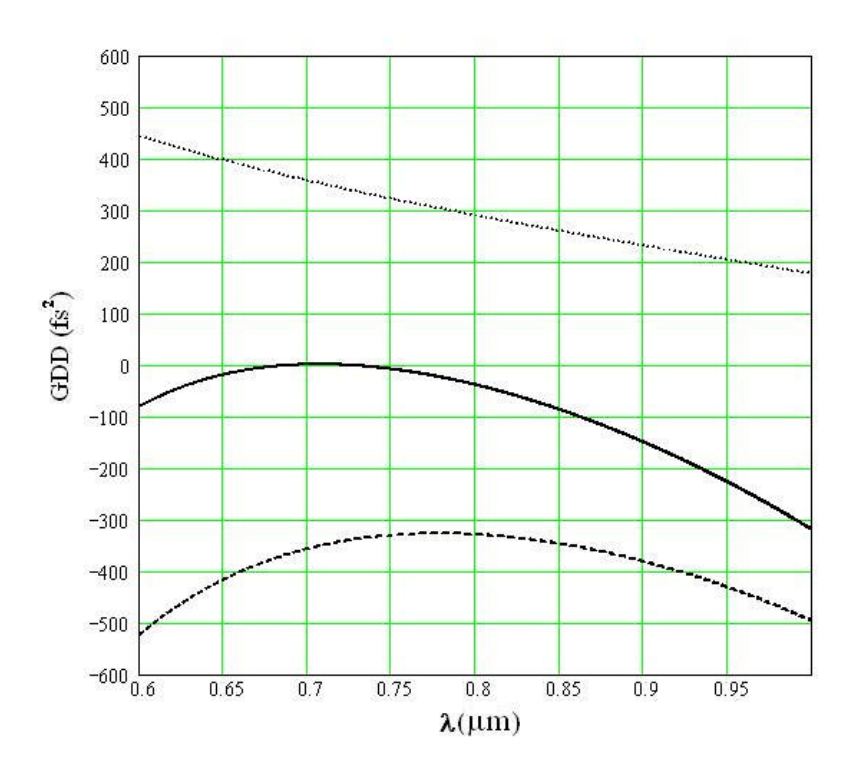


Figure 3.8: GDD (fs²) versus wavelength (_m) for: 5-mm long Ti:sapphire crystal (dotted line), fused-silica prism pair with parameters L=620 mm and e=5 mm (dashed line), and the residual net GDD (solid line) arising from the balance between positive GDD of the crystal and negative GDD of the prism pair.

In fact, stable pulsed operation of the laser exactly at the zero GDD boundary is also impossible, since higher order terms in the group delay dispersion (not included in the above analysis) lead to pulse distortions and eventually tend to break up the pulse. Moreover, there is an extra chirp arising from Kerr-nonlinearity of the active medium. Therefore the setting of the laser to the optimum stable condition of the shortest pulse can be accomplished by a slight overcompensating of GDD. As it is very complicated to be estimated in numerical way, the extra amount of negative GDD needed for the overcompensation is found by slight tuning of dispersion below zero-GDD in the laser. Practically the tuning can be easy performed by moving one of the prism along its axis of symmetry, thus the parameter e of the expression 2.16 can be varied. Simultaneously it also results in changing of central wavelength.

3.3.2 Stability zones of the laser.

The optical resonator must be constructed in such a way that upon several passes through the resonator, the radiation remains captured, and amplification of the radiation is accomplished. This condition results in ranges of the geometrical cavity parameters, which allow lasing. The stability zones for this configuration can be calculated making use of the ABCD matrix formalism. For a full account on this matter the reader is referred to Ref [16]. The calculated stability zones of a four-mirror Z-folded cavity are depicted in the Figure 3.9. The calculations are performed for the actual experimental setup parameters, (length of the cavity arms, and curvatures of the concave mirrors). The running variable in the calculations is formed by the variation of distance between the two curved mirrors M3 and M4 (figure 3.2). In the Figure 3.9 two regions of stability can be distinguished. The appearance of an instability gap separating the stability zones is a result of a laser configuration with unequal arms length ($L_1 \neq L_2$, see fig.3.1, $L_1 = l_1 + l_2 + l_3$). The width of the gap then can be estimated as [13]:

$$\delta = \frac{R^2 (L_1 - L_2)}{(2L_1 - 2R)(2L_2 - R)}$$
(3.3)

while the width of the stability zones can be taken as [13]:

$$Z = \frac{R^2}{4L_1 - 2R} \tag{3.4}$$

where R is curvature radius of the concave mirrors. According to the required prism spacing and a total dimension limitation, the long arm length L_I is set at 860 mm while the short arm length L_2 is set at 570 mm. The total cavity length is thus about 1535 mm (taking into account the spacing between the curved mirrors). In the calculations the non-linear (Kerr) phenomena is initially neglected, the results are thus predicted for cw-laser operation.

For simple modeling the self-focusing action of the Ti:sapphire crystal, a positive lens is placed inside the Ti:sapphire crystal [13]. With inclusion of the Kerr-lens, significant changes in the location of the stability zones are found. Especially the second stability zone shifts to smaller values. Although the strength of the Kerr-lens is taken somewhat arbitrarily, from this simple analysis one can already conclude that when the laser operates near the inner borders of the stability zones, a preferential gain should exist for the high-intensity mode-locked radiation. Note that this effect is

only based on the cavity stability conditions in combination with the effect of self-focusing, no effect of an aperture on the cavity beam is included here. Sometimes such mechanism is also called gain-guiding due to the fact that the nonlinear active medium spatially reshapes cavity modes. So, to switch the laser to pulsed regime, the laser resonator can be aligned to operate in either the first (I) or second (II) stability zone, but should in both cases be aligned exactly at the inner border. In this case cw-lasing is hardly supported by transient stability conditions while high intensive pulsed radiation causing Kerr-focusing can be preferable. In addition, under certain conditions (when the pumping beam is focused so that its waist diameter is close to the waist diameter of generated radiation), the combination of self-focussing and gain saturation (gain-aperturing) can be used to produce a differential gain that favours the growth of short pulses and eliminates cw oscillations [13,14].

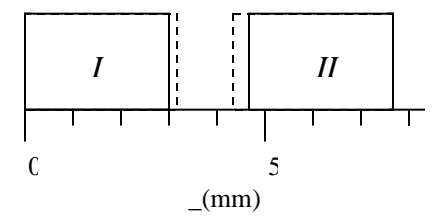


Figure 3.9: Stability zones of the laser. _ is extension of the distance between the concave mirrors from the point corresponding to the confocal arrangement. The dashed lines mark the boundaries of the stability zones in case an additional (Kerr) lens is simulated.

One should also take into account that as a result of the presence of the Brewster angle of the Ti:sapphire crystal, some astigmatism is introduced in the cavity. Although, in the presented cavity design, in contrast to a real Z-folded cavity, astigmatism cannot be completely compensated, one can minimize it by tilting the folding mirrors M3 and M4 to a certain angle extantion. Based on the expressions presented by Kigali *et al.* [17], the angle _ (Figure 3.1) can be calculated as:

$$\theta = 2\arccos - C/2 + \sqrt{(C/2)^2 + 1}$$
 (3.5)

$$C = \frac{t(n^2 - 1)\sqrt{(n^2 + 1)}}{n^4 R}$$
 (3.6)

where t and n are the thickness and the refractive index of the Brewster-angled medium; R is the radius of curvature of the folding mirrors. With a refractive index of n=1.76, a thickness of t=5

mm and a curvature radius of R=100 mm, a folding angle of $_=17^{\circ}$ is found. In fact, the mirror M3 is tilted at the found angle; the mirror M4 is tilted at a minimal angle allowed by the cavity geometry.

3.4. Operating characteristics of the mode-locked laser

The laser produces up to 1 Watt of cw-radiation centered around 830 nm upon 6 Watt of pump radiation, when the cavity is aligned for optimal cw-regime (at the center of stability zone). So, a conversion efficiency (absorbed pump power over laser power) of more than 20% (output coupler is T=10%) can be easily achieved in the cw-regime. To act in mode-locked regime the laser must be aligned at an inner boundary of the stability zones. For both the predicted positions (inner borders of the stability zones, Figure 3.9), mode-locking was experimentally verified. The most stable mode-locking was found at the inner boundary of the stability zone I. No hard aperture was needed when operated at this position. When the laser operates near the inner boundary in the first (I) stability zone, it generates a cw-output power of 480 mW. Upon the mode-locking of the laser a significant increase in the laser power is observed (up to 800 mW) as a result of a preferential gain effect for the short pulse mode as discussed in the previous Section 3.3.2. Mode-locking can easily be started by a quick push of the spring-loaded mount of the prism P1 (Figure 3.2), due to a strong dispersive perturbation for CW oscillation. While the system operates in CW-regime we observe a fairly narrow optical spectrum. But, when mode-locking is started, the optical spectrum is extended more than 5 times, due to SPM of pulse radiation in the active medium. The measured FWHM of the spectrum is 45 nm (19 THz) and the central wavelength can be set within the range 855 ÷880 nm. Typical traces of optical spectrum of pulse radiation is shown in the fig.3.10. The change of the central wavelength when the laser is switched from cw to pulsed regime can be explained by the frequency dependent behavior of net cavity GDD (Figure 3.8), and probably the pulse generation appears at the frequency corresponding to a really sufficient GGD compensation. Due to this mechanism, a tuning of the wavelength in a small range can be performed, by moving the prism P1 along its axis of symmetry. However it may also be accompanied with diffraction losses on the side of the prism. In fact, as it is applied to a side of the pulse spectra, such losses cause a spectral

clipping of pulses and thus result in a temporal broadening of pulses. So, in principle, to obtain optimal conditions at the desirable wavelength, a tuning of the net GDD should be performed by a tuning of the prism spacing. Practically, it requires complex adjustments. To study the spectrum of intermode beats of a femtosecond comb we use a high-speed photo detector together with a wideband spectrum analyzer. For instance, a typical spectrum of intermode beat signal is shown in fig.3.11. As the total cavity length is set at approximately 1535 mm, the laser operates with repetition rate (i.e. intermode frequency spacing) of 97.7 MHz. A control of this frequency can be provided by a translation of the mirror M1. An explicit tuning (within 0.5 MHz) can be performed without additional intracavity realignments. From the data above, one can estimate that the generated spectral continuum consists (at FWHM) of more then 193 000 longitudinal modes. The pulse duration estimated from measurement by the interferometeric autocorrelator is about 35 fs. An example of autocorrelation function is shown in fig.3.12.

The measured value of the time-bandwidth product is equal to t =0.65 and two times larger than the expected value for an ideal sech shaped pulse (0.315). This is a result of the non-sech shape of intensity profile, which leads in general to a larger value of the time-bandwidth product (Gauss: t ==0.441). Furthermore, the thickness of 9 mm of the output coupler made of BK7 material introduces extra GDD of 350 fs² for pulses passing through it and thus results in temporal broadening of pulses. So, if one's aim is to get minimal pulse duration the output coupler should be replaced with thin one or an external prism GDD compensator should be used. As our goal is not a record of the shortest pulse duration, we propose only optimizing of cavity net GDD to minimize residual pulse chirp and, by this, to reduce pulse duration.

In conclusion

Thanks to unique properties of the radiation in both spectral and time domain the constructed laser seems to be a very attractive instrument for different kind of new investigations. For example, now this laser is being used to irradiate thin InSn plates in order to induce a reflectivity change in the FIR region by photoelectric effect. This technique was already tested, using a nanosecond laser [18]. The goal is to obtain the modulation of a FIR laser radiation at the femtosecond laser repetition rate; hence producing side bands about 100 MHz far from the FIR laser frequency. In such way it

may be possible to reach the frequency corresponding to an interesting (for metrology) atomic transition in Ca.

We also propose to stabilize a spectral comb of the femtosecond laser by a control of the pulses repetition rate. An active stabilization, that is, a phase-lock of the mode beat frequency of a femtosecond laser to the frequency of a stable radio oscillator, seems to be the most efficient approach [5].

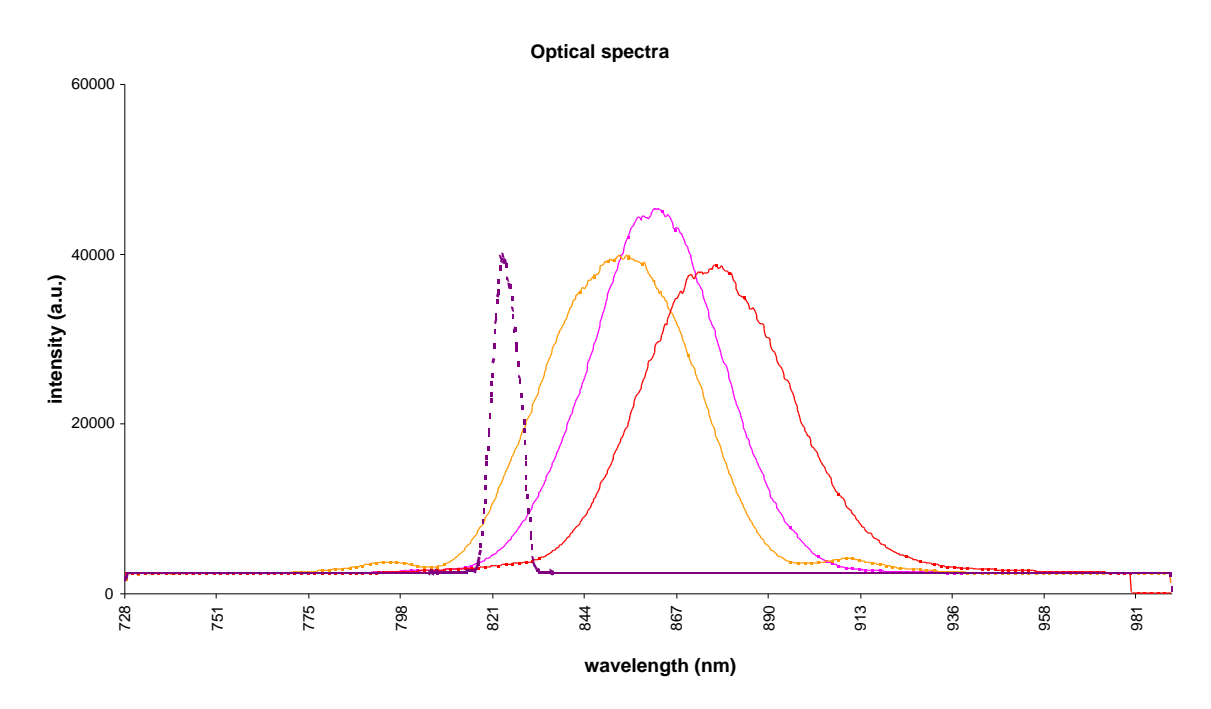


Figure 3.10. Traces of optical spectrum. (dotted line is a spectrum of a non-mode-locked regime).

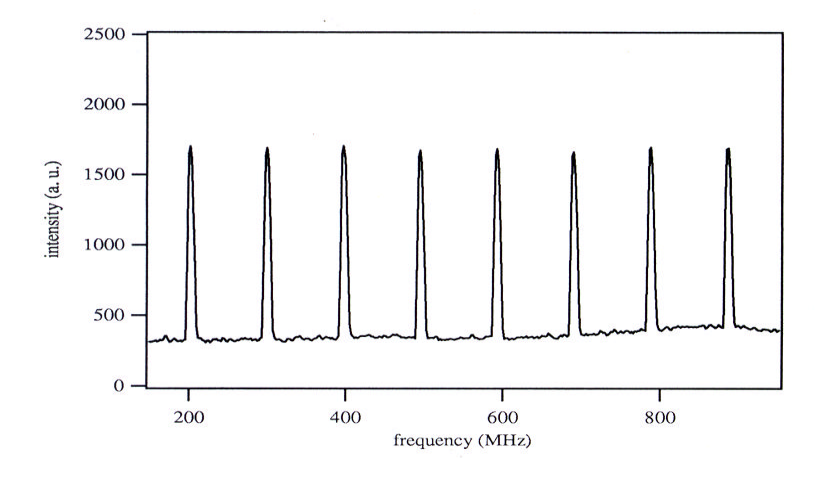


Figure.3.11. Spectrum of intermode beat signal.

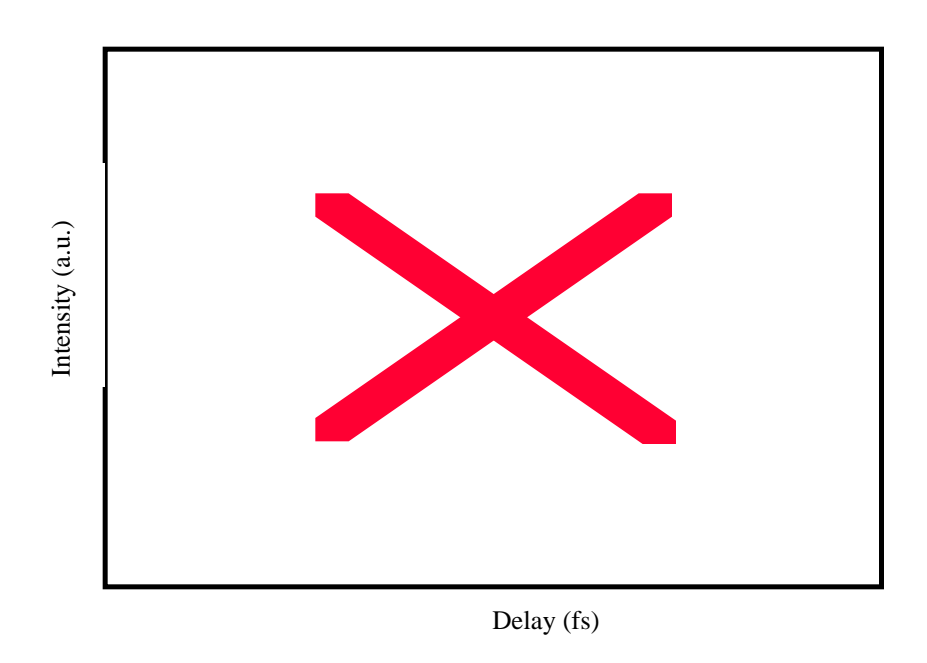


Figure.3.12. Interferometric autocorrelation trace.

References

- [1] Paolo Foggi, Laura Bussotti, and Frederik V. R. Neuwahl *Photophysical and photochemical applications of femtosecond time-resolved transient absorption spectroscopy* International journal of photoenergy, Vol.3, 103 (2001)
- [2] Wayne H. Knox Ultrafast Technology in Telecommunications IEEE journal on selected topics in quantum electronics, Vol. 6, No.6 (2000)
- [3] Th. Udem, J. Reichert, R. Holzwarth, T.W. Hansch. *Accurate measurement of large optical frequency differences with a mode –locked laser* Opt. Lett., vol.24, N 13, 991 (1999).
- [4] Diddams S.A., Jones D.J., Ye J., Cundiff S.T., Hall J.L, Ranka J.K., Windeler R.S., Holzwarth R., Udem T., and Hansch T.W. Direct link between microwave and optical frequencies with a 300 THz femtosecond laser comb Phys. Rev. Lett., vol. 84, pp. 51025105, (2000)
- [5] S.N. Bagayev, S.V. Chepurov, V.M. Klementyev, D.B. Kolker, S.A. Kuznetsov, Y.A. Matyugin, V.S. Pivtsov, V.F. Zakharyash *Application of Femtosecond Lasers for the Frequency Synthesis in Radio-Optical Ranges and for the Creation of an Optical Clock* Laser Phys. V.11, n10, pp. 1094-1097 (2001)

- [6]R. Holzwarth, J. Reichert, Th. Udem, and T. W. Hänsch A New Type of Frequency Chain and Its Application to Optical Frequency Metrology Laser Physics, Vol. 11, No. 10, 2001, pp. 1100–1109.
- [7] O. Svelto Principles of lasers 1989
- [8] G. Cerullo, S. De Silvestri, V. Magni, and L. Pallaro, *Resonators for Kerr-lens mode-locked femtosecond Ti:sapphire lasers* Opt. Lett. Vol.19, Issue 11, 807–809 (1994).
- [9] D.H. Sutter, L. Gallmann, N. Matuschek, F. Morier-Genoud, V. Scheuer, G.Angelow, T. Tschudi, G. Steinmeyer, U. Keller Sub-6-fs pulses from a SESAM-assisted Kerr-lens modelocked Ti:sapphire laser: at the frontiers of ultrashort pulse generation Appl. Phys. B 70 [Suppl.], S5–S12 (2000)
- [10] Christian Spielmann, Peter F. Curley, Thomas Brabec, and Ferenc Krausz *Ultrabroadband femtosecond lasers*. IEEE Journal of quantum electronics, vol.30, N.4, 1100 (1994).
- [11] V. S. Grigoryan Formation of solitary pulses in an amplifying nonlinear medium with dispersion *JETP Lett.*, v. 44, No. 10, pp. 575-579 (1986).
- [12] D ARIVUOLI Fundamentals of nonlinear optical materials PRAMANA journal of physics (Indian Academy of Sciences) Vol. 57, No. 5 & 6, pp. 871–883 (2001)
- [13] A.A. Angelutz, D.P. Krindach, A.V. Pakulev, V.I. Surmii, Kerr lens modulation processes in femtosecond Ti:sapphire laser SPIE Proceedings Vol. 2095, pp.73-76 (1994)
- [14] A. A. Angeluts, D. Yu. Kobelev, D. P. Krindach, A. V. Pakulev *Self-modulation of the unsaturated gain in a femtosecond Ti: sapphire laser* Quantum Electronics Vol. 25, No. 11, pp. 1063-1066 (1995)
- [15] Francois Salin, Alain Brun Dispersion compensation for femtosecond pulses using high index prisms J. Appl. Phys. Vol. 61, No.10 (1987)
- [16] A. Gerrard, JM Burch Introduction to Matrix Methods in Optics (Any editions)
- [17] H.W. Kogelnik, E.P. Ippen, A. Dienes, C.V. Shank IEEE J. Quantum. Electr. 8, 373 (1972).
- [18] A. Bertolini, G. Carelli, N. Ioli, C. A. Massa, A. Moretti, A. Ruffini and F. Strumia *Generation of monochromatic nanosecond pulses in the FIR region*J. Phys. D: J. Appl. Phys.33, pp.345-348 (2000)